Analytica Chimica Acta 1150 (2021) 238177

Contents lists available at ScienceDirect

Analytica Chimica Acta

journal homepage: www.elsevier.com/locate/aca

Dual-emission fluorescence biosensing of vancomycin based on AIEgen–peptide conjugates and aptamer-modified Au nanoclusters

Fangya Mu , Junqing He , Fang Fan , Guoyue Shi *

Department of Chemistry, School of Chemistry and Molecular Engineering, East China Normal University, Dongchuan Road 500, Shanghai, 200241, China

HIGHLIGHTS

- An AIEgen-Peptide/AuNCs-apt fluorescent sensor was developed for Van detection.
- The system showed good sensitivity and selectivity in the range of 0.01 −100 μg mL^{-1}.
- Dual-emitting ratiometric fluorescent sensing of Van was demonstrated.
- The sensor effectively distinguishes Van from glycopeptide antibiotics.

GRAPHICAL ABSTRACT

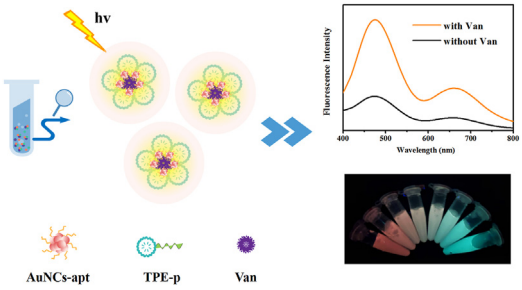

ARTICLE INFO

Article history:
Received 6 November 2020
Received in revised form
21 December 2020
Accepted 22 December 2020
Available online 16 January 2021

Keywords:
Vancomycin
AIE luminogens
Au nanoclusters
Dual-emission biosensor platform

ABSTRACT

Precise doses of antibiotics are necessary to prevent bacterial drug resistance. Although fluorescent sensors are promising for quantitative analyses of antibiotics, improvements in feasibility, selectivity, and sensitivity are needed. In this study, a dual-emission fluorescence biosensor platform was developed for simple, selective, and sensitive determination of vancomycin (Van) based on a peptide conjugated with blue-emitting aggregation-induced emission luminogens (AIEgen) and aptamer-modified red-emitting gold nanoclusters (AuNCs-apt). The peptide and aptamer together recognized Van with high affinity, thus changing the fluorescence intensity at 470 nm and 650 nm, respectively. This platform displayed excellent linear correlation between the fluorescence response and a Van concentration ranging 0.01 −100 μg mL^{-1}, and the limit of detection (LOD) was 2.79 ng mL^{-1}. In addition to the ability to accurately distinguish Van from glycopeptide antibiotics, the newly developed biosensor allowed for naked-eye detection of 1 μg mL^{-1} Van. These results and those of serum samples and microdialysate samples support the application of this newly developed method for Van monitoring and clinical diagnosis.

1. Introduction

Owing to the recent increase in antibiotic-resistant bacteria, the broad-spectrum antibiotic vancomycin (Van) is widely used in clinical settings. However, Van is potentially nephrotoxic and ototoxic, especially when used in combination with other ototoxic or nephrotoxic agents and in patients with renal impairment. It is necessary to monitor Van levels to ensure that the target therapeutic range is achieved. To provide a reliable basis for the rational clinical use of drugs [1], a high efficacy and low incidence of toxicity are necessary [2]. It is therefore important to monitor drug levels in the blood and promptly adjust antibiotic dosing regimens. Most conventional detection methods for Van use high-performance liquid chromatography (HPLC) [3,4] and ELISA [5]. Fluorescence

* Corresponding author.
E-mail address: gyshi@chem.ecnu.edu.cn (G. Shi).

https://doi.org/10.1016/j.aca.2020.12.052
0003-2670/

detection is a rapid, stable, sensitive, and cost-effective method. Several fluorescent sensors for Van detection have been reported [6,7]. However, innovative methods for rapid Van detection are still needed, and a reliable fluorescent biosensor for serum Van would be clinically significant.

Aptamers are small nucleic acid molecules interacting with target molecules with high specificity and affinity. Plaxco et al. used aptamer-based sensors for sensitive electrochemical detection of Van [8]. High-specificity aptamers can be used to construct fluorometric aptasensors for Van. Furthermore, gold nanoclusters (AuNCs) are widely used as biosensors owing to their stable fluorescence, excellent photostability, high emission rate, and excellent biocompatibility [9,10]. Aptamer-stabilized AuNCs have been studied extensively owing to their high affinity to single-stranded DNA [11,12]. Moreover, size-dependent fluorescence and color tunability are beneficial properties for biological imaging and sensing [13].

To resolve aggregation-caused quenching (ACQ), an issue associated with traditional fluorescent materials, aggregation-induced emission (AIE) has attracted considerable attention [14]. Compared with traditional ACQ fluorescent materials, AIE materials have various advantages, including high signal-to-noise ratio owing to low background emission, high sensitivity, and strong anti-bleaching ability. AIE molecules are generally non-emissive in their molecular dissolved state; however, they can be induced to display high luminescence efficiency in the aggregated or solid state [15]. Peptides conjugated with AIE luminogens (AIEgens) interact with biotargets with high specificity and high affinity. AIE-peptide probes have been designed to monitor apoptosis [16], detect proteins and enzymes [17], and visualize specific organelles [18] and tissues [19].

This study aimed to develop a novel dual-emission fluorescence biosensor platform for the sensitive, rapid, and specific detection of Van at a single excitation wavelength. Fluorescent AIE and AuNCs were synthesized and conjugated with a specific peptide and aptamer to capture Van, respectively. As the concentration of Van increased, dual-emission fluorescence peaks centered at 470 and 650 nm, respectively, while a color change from red to orange and blue was clearly observed under UV light. We provide a novel demonstration of the convenient detection of Van by the naked-eye. Moreover, the method had a low LOD and wide detection range of 0.01–100 μg mL^{-1}. Therefore, the present newly developed method may be potentially applicable in the public health and clinical settings.

2. Materials and methods

2.1. Materials and reagents

Van, teicoplanin (Tei), $HAuCl_4 \cdot 3H_2O$ (hydrogen tetrachloroaurate trihydrate), and bovine serum albumin (BSA) were obtained from Sigma-Aldrich (St. Louis, MO, USA). 1-ethyl-3-(3-(dimethylamino)propyl) carbodiimide hydrochloride (EDC) and *N*-Hydroxysuccinimide sodium salt (NHS) were obtained from Macklin Inc. (Shanghai, China). NaOH, $CuSO_4$, and sodium ascorbate were purchased from Aladdin (Shanghai, China). A Van aptamer [8] (5′–NH_2– CGAGGGTACCGCAATAGTACTTATTGTTCGCCTATTGTGGG TCGG-3′) was synthesized and purified by Shanghai Sangon Biotechnology Co. Ltd. (Shanghai, China). e (Propargylamine)K(Ac) aa (where e represents D-Glu and a represents D-Ala) peptides were provided by ChinaPeptides Co., Ltd. The Van ELISA Kit was obtained from Jining Shiye Co. Ltd. (Shanghai, China). The 1 × PBS contained NaCl (137 mM), KCl (2.7 mM), Na_2HPO_4 (10 mM), and KH_2PO_4 (1.8 mM). All chemicals and reagents were of analytical reagent grade and were used as received without further purification. Double deionized water was purified using a Milli-Q Plus Water Purification System (Millipore, Billerica, MA, USA).

2.2. Instruments

Fluorescence spectroscopy was performed using the Infinite M200 microplate reader (TECAN, Männedorf, Switzerland) in a 384-well black microplate (Corning, Inc., Corning, NY, USA) (excitation wavelength of 330 nm). The molecular weight was detected by Fourier transform mass spectrometry (Bruker Daltonics Inc.). Transmission electron microscopy (TEM) images were obtained using a transmission electron microscope (JEM-2100F; JEOL, Tokyo, Japan) operated at 200 kV. Dynamic light scattering (DLS) and zeta potentials were measured using a Malvern Zetasizer Nano ZS3600.

2.3. Synthesis of TPE-p

TPE-p (TPE-peptide) was synthesized as follows. Alkyne-functionalized peptide e (Propargylamine)K(Ac)aa (19.9 mg, 40 μmol) and TPE-N_3 (Azide-functionalized tetraphenylethene) (15.5 mg, 40 μmol) were dissolved in a mixture of dimethyl sulfoxide (DMSO) and water (v/v = 5/1, 2.0 mL). The “click” reaction was initiated with a catalyst system of $CuSO_4$ (12.8 mg, 80 μmol) and sodium ascorbate (31.7 mg, 160 μmol). The reaction proceeded through continuous agitation for another 24 h at 22–25 °C. The crude product was purified by HPLC and lyophilized under vacuum to yield the probe (8.5 mg, 24% yield) as a white powder. TPE-p was characterized by Fourier transform mass spectrometry: FTMS (ESI, positive) *m/z* $[M + H]^+$ calcd 884.44537; found 884.44257 (see Fig. S1).

2.4. Preparation of AuNCs-apt

The BSA-AuNCs were synthesized using a previously described method [20]. Aptamer-modified AuNCs-apt was prepared by amide condensation. Briefly, 4 μL of BSA-AuNCs was added to 196 μL of PBS, followed by the addition of EDC (0.56 mg) and NHS (0.32 mg) with continuous stirring at 37 °C for 30 min. Thereafter, 10 μM Van aptamer (20 μL) was added to the solution and maintained at 37 °C for the condensation reaction. The BSA-AuNCs solution was further purified through dialysis for 24 h, using a 1000 MWCO dialysis membrane.

2.5. Fluorescence measurement

TPE-p was dissolved in DMSO to prepare a stock solution with a concentration of 2.0 mM and diluting to final concentration with PBS. TPE-p (10 μM, DMSO/water (v/v = 1:199)) was mixed with AuNCs-apt (100 nM). Thereafter, Van at various concentrations (0, 0.01, 0.02, 0.05, 0.1, 0.2, 0.5, 1, 2, 5, 10, 20, 50, and 100 μg mL^{-1}) was added to the mixture and incubated for 30 min at 22–25 °C. The fluorescence intensity of the solution was measured at an excitation wavelength of 330 nm and emission wavelength of 400–800 nm.

2.6. Detection of real samples

Blood samples were collected from adult male Sprague–Dawley rats (200–250 g, SLAC Laboratory Animal Co. Ltd., Shanghai, China) and allowed to coagulate at room temperature, followed by centrifugation at 5000 rpm for 15 min to obtain serum samples. Then, Van was added at various concentrations to obtain spiked samples. The pharmacokinetics of Van was investigated in blood, using microdialysis in a rabbit animal model (Three adult male New Zealand rabbits (2–2.5 kg, JSJ-Lab Co., Ltd., China)). Details of in vivo microdialysis experiments are provided in the Supporting

Information. All animals were maintained on a 12-h light-dark cycle in a temperature-controlled environment (22 ± 1 °C) with *ad libitum* access to food and water. All procedures involving animals were approved by the Animal Ethics Committee of the East China Normal University, China (No. Rb 20190701).

2.7. Method comparison

Van concentrations in the serum samples were analyzed with the proposed method and the Van ELISA Kit in accordance with the manufacturer's instructions. Passing-Bablok regression analysis (MedCalc, Ostend, Belgium) was performed to evaluate the agreement between the two different analytical methods. The correlation coefficient, intercept, and slope were estimated using Passing-Bablok regression analysis with 95% confidence intervals (95% CI).

3. Results and discussion

3.1. Characterization of TPE-p and AuNCs-apt

Benzene, 1-(azidomethyl)-4-(1,2,2-triphenylethenyl) (TPE-N_3) was synthesized according to previously described method [16]. The ^{1}H spectrum of TPE-N_3 is shown in Fig. S2. The TPE-p synthesis route is shown in Scheme S1. The AIEgen is nonfluorescent in good solvents, but displays intense fluorescence emission when aggregated in poor solvents. As shown in Fig. S3, TPE-N_3 was hydrophobic, with intense fluorescence as an aggregate in a mixture of DMSO/water (v/v = 1/199), and TPE-p was largely nonfluorescent in the same medium owing to its high hydrophilicity. In the presence of Van, TPE-p displays strong fluorescence signals. For the TPE-modified peptide, the blue-shift in the fluorescence spectrum can be attributed to the blockade of the non-radiative decay pathways by restricting intramolecular rotations [21]. TPE-N_3 was determined by DLS measurement to be composed of aggregates with an average size of 105 nm in aqueous media (Fig. S4A). However, TPE-p could not be detected by DLS because of its high hydrophilicity compared to that of hydrophobic TPE-N_3.

AuNCs-apt were synthesized by an amide condensation reaction between BSA-AuNCs and the aptamer [22]. TEM revealed that the resulting AuNCs-apt were pseudo spherical particles with an average size of 2.15 nm (Fig. 1A). As shown in Figs. S4C and S4D, the average hydrodynamic diameter, as determined by DLS, increased from 7.4 nm (AuNCs) to 11.2 nm (AuNCs-apt). As shown in Fig. S5, the zeta potential values were −8.2 mV for AuNCs and −12.7 mV for AuNCs-apt. Aptamer conjugation resulted in a more negative zeta potential, proving the successful formation of AuNCs-apt. The zeta potential for the conjugate of TPE-p/AuNCs-apt/Van was substantially higher than those of TPE-p and AuNCs-apt, indicating that TPE-p and AuNCs-apt can successfully capture Van. As observed by TEM (Fig. 1B and C), the conjugate of TPE-p/AuNCs-apt/Van had the average diameter of 200 nm and were homogeneous spherical particles. Furthermore, DLS data indicated that aggregates were formed with average hydrodynamic diameters of 326 nm (Fig. S4B).

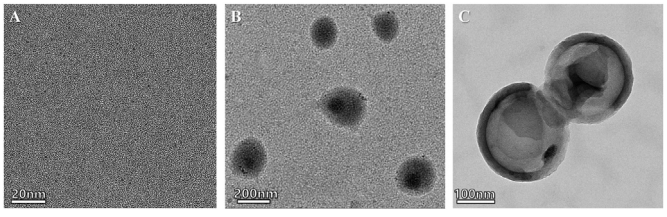

Fig. 1. (A) TEM image of AuNCs-apt. (B) and (C) TEM image of TPE-p/AuNCs-apt/Van.

3.2. Principle for Van detection

Fig. 2A shows the normalized emission spectra for TPE-p, AuNCs-apt, and Van in the TPE-p AuNCs-apt system. The maximum emission wavelengths of TPE-p and AuNCs were 470 nm and 650 nm, respectively, at a single excitation wavelength of 330 nm. Furthermore, the mixed emission spectra for TPE-p and AuNCs did not overlap; this lack of spectral overlap ensures the successive potential for Van quantification. For excitation at 365 nm (under UV light), the corresponding photographs are shown in Fig. 3A, in which TPE-p and AuNCs-apt show blue and strong red emission, respectively.

The TPE-p and AuNCs-apt dual-emission fluorescence sensing platform for Van is illustrated in Scheme 1. The D-Ala-D-Ala of TPE-p and aptamer molecules exhibit highly specific binding to Van. Our results supported the feasibility study of the proposed system for measuring the fluorescence intensity of Van in different solution systems. As shown in Fig. 2B, TPE-p and AuNCs-apt strands were in the free state with very weak fluorescence in the absence of Van and aggregated to form TPE-p-Van-AuNCs-apt in the presence of Van with a sharp increase in fluorescence. However, when a random DNA sequence (AuNCs-Rapt) replaced the aptamer specific to Van, there was only a slight but non-significant increase in fluorescence intensity. Moreover, when Van was replaced with Tei, the fluorescence intensity at 470 nm increased, with no change in fluorescence intensity at 650 nm. The glycopeptides teicoplanin and Van both act by binding to C-terminal D-Ala-D-Ala. However, using the aptamer with high affinity and specificity for Van, our dual-emission probes can effectively distinguish between glycopeptide antibiotics.

3.3. Optimization of detection conditions

For optimal sensing performance, the concentrations of TPE-p and AuNCs-apt, pH, temperature, and reaction time were optimized. As shown in Figs. S6A and S6B, the fluorescence signal change ΔF ($\Delta F = (F-F_0)/F_0$, where F_0 and F are fluorescence intensities in the absence and presence of 50 μg mL^{-1} Van at 470 nm and 650 nm, respectively) for TPE-p increased from 5 to 50 μM and that for AuNCs-apt increased from 20 to 200 nM. When the concentrations of TPE-p and AuNCs-apt were 10 μM and 100 nM, respectively, the maximal changes in fluorescence intensity of the system were observed. pH is an important factor influencing fluorescence spectra. As shown in Fig. S6C, the optimal pH value for Van quantification was 7.4. Considering the potential application of the probe to biological systems, PBS (pH 7.4) was selected for subsequent experiments. Temperature hardly influenced Van detection; therefore, experiments were performed at ambient temperature (25 °C) (Fig. S6D). The time required to obtain a relatively stable signal was optimized. As shown in Fig. S6E and a steady change in

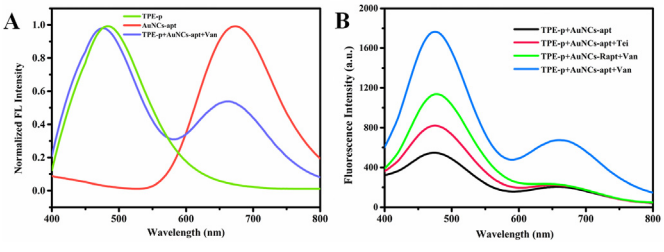

Fig. 2. (A) Fluorescence emission spectra for TPE-p (green line), AuNCs-apt (red line), and TPE-p/AuNCs-apt/Van (blue line). (B) Fluorescence emission spectra for TPE-p/AuNCs-apt, TPE-p/AuNCs-apt/Tei, TPE-p/AuNCs-Rapt/Van, and TPE-p/AuNCs-apt/Van systems.

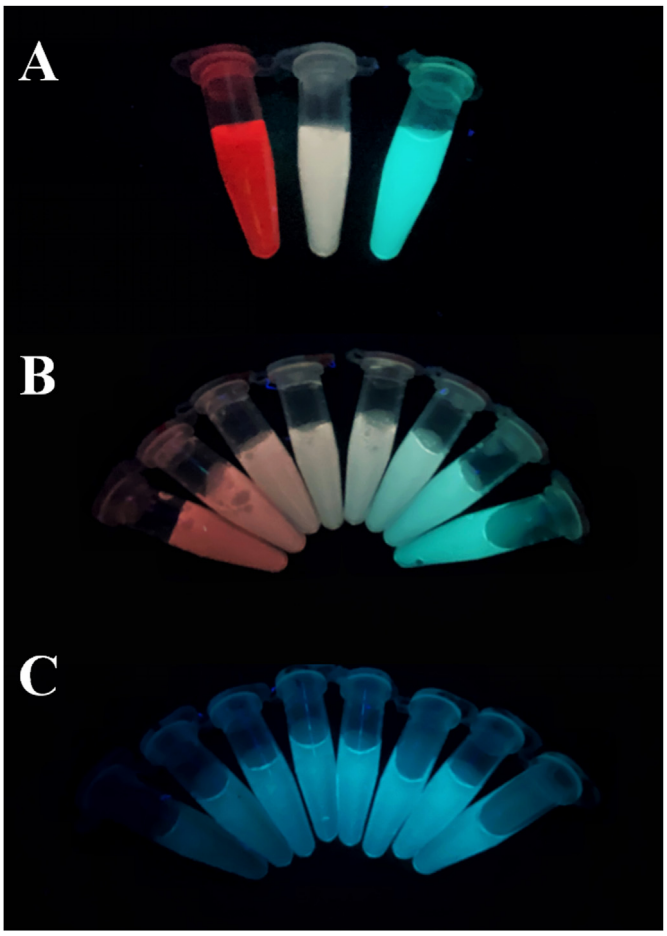

Fig. 3. Photograph of the semiquantitative determination of Van under UV light. (A) Fluorescence for TPE-p, TPE-p/AuNCs-apt/Van, AuNCs-apt (from left to right). (B) The change in fluorescence intensities in the TPE-p/AuNCs-apt system under different concentrations of Van (from left to right): 0, 1, 2, 5, 10, 20, 50, and 100 μg mL^{-1}. (C) Fluorescence detection in the TPE-p system with different concentrations of Van (from left to right): 0, 1, 2, 5, 10, 20, 50, and 100 μg mL^{-1}.

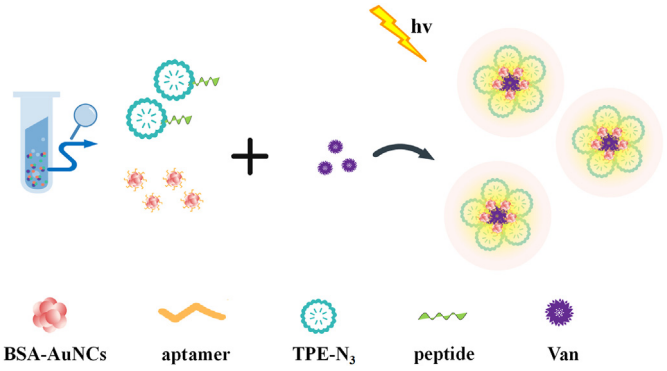

Scheme 1. Schematic illustration of the sensing platform for detecting Van.

fluorescence at both 470 nm and 650 nm was observed upon Van supplementation. The fluorescence of TPE-p increased rapidly and peaked at 10 min. The fluorescence increase for AuNCs-apt was relatively gradual and plateaued within 30 min and stabilized thereafter. Therefore, an incubation time of 30 min was used for subsequent experiments. Furthermore, as shown in Fig. S6F, the fluorescence response of TPE-p/AuNCs-apt/Van towards Van was stable because the fluorescence signal was nearly unchanged when

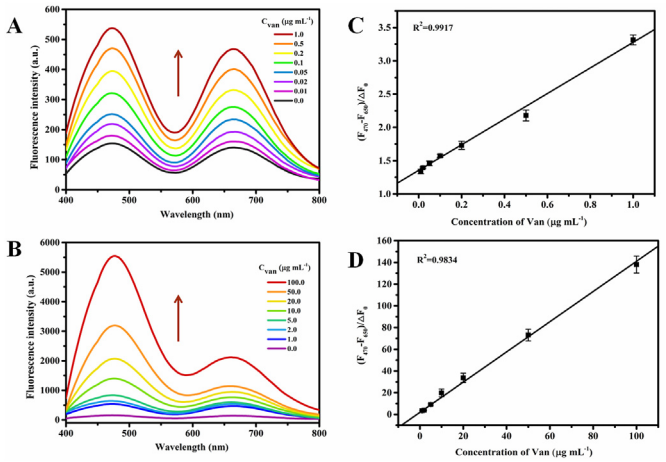

Fig. 4. Fluorescence spectra for the assay in the presence of different Van concentrations ranging (A) 0.01–1 μg mL^{-1}, (B) 1–100 μg mL^{-1}. Corresponding linear curve for Van detection in the range of (C) 0.01–1 μg mL^{-1}, (D) 1–100 μg mL^{-1}.

used as the probe to detect Van for five consecutive days, indicating high system stability.

3.4. Quantitative detection of Van

To explore the practical application of our dual-emission sensor platform, quantitative analysis of Van was performed. As shown in Fig. 4A and C, at optimum TPE–p and AuNCs-apt concentrations (i.e., 10 μM and 100 nM, respectively), the fluorescence intensities gradually changed at wavelengths of 470 nm and 650 nm as the concentration of Van increased from 0.01 to 100 μg mL^{-1}. A significant linear association was obtained between the fluorescence intensity and the concentration of Van in two concentration ranges (Fig. 4). In particular, good linearity ($(F_{470}-F_{650})/\Delta F_0 = 1.92 + 1.35C_{van}$, $R^2 = 0.9917$ (Fig. 4C) was observed in the lower concentration range (0.01–1 μg mL^{-1}). Furthermore, a linear association was observed in the concentration range of 1–100 μg mL^{-1} ($(F_{470}-F_{650})/\Delta F_0 = 1.39 + 1.89C_{van}$, $R^2 = 0.9834$ (Fig. 4D). Note that $\Delta F_0 = F_{0(470)} - F_{0(650)}$, where $F_{0(470)}$, F_{470}, $F_{0(650)}$, and F_{650} are the fluorescence intensities at 470 nm and 650 nm in the absence and presence of Van, respectively. The LOD was 2.79 ng mL^{-1} (LOD = 3 standard deviations/slope, n = 10).

The newly developed method can be utilized for quantitative detection of Van. The fluorescence intensity ratio of blue-emissive TPE-p and red-emissive AuNCs can yield obvious color changes for visual detection of various concentrations of Van from 1 to 100 μg mL^{-1}. The probe changes from red to orange and blue under UV light (Fig. 3B). Using only TPE-p for detection (Fig. S7), as the concentration of Van increased (1–50 μg mL^{-1}), the fluorescence intensity at 470 nm increased. The working range was smaller than that of our dual-emission sensor platform. Furthermore, as shown in Fig. 3C, the color change of TPE-p in response to the addition of Van was not obvious. The dual-emission sensor platform uniquely facilitated the visual detection of Van under UV light. As shown in Table 1, the fluorescence sensor was compared with previously reported sensors that target Van. Dual-emission fluorescence is superior to other sensors in terms of LOD and visual detection. Our probes were able to effectively distinguish between glycopeptide antibiotics for specific Van detection.

3.5. Selectivity of the detection strategy

To confirm the selectivity of the detection strategy, different

Table 1
Comparison of the performance of analytical methods for Van quantification.

Method	Material	Linear range	LOD	Sample type	Ref
E-AB	Aptamer	6–35 μM	Not given	plasma	[8]
HPLC	–	2–50 μg mL^{-1}	Not given	serum	[23]
LC-MS	–	Not given	0.3 μg mL^{-1}	plasma	[24]
DFPA	Fluorescent labeled peptides	0.5–4 μM	0.5 μM	human blood	[6]
Fluorescence	Organic fluorescent probe	0.25–32 μM	96.9 nM	human serum	[25]
Fluorescence	CdTe quantum dots	1.534 ng mL^{-1} to 20 μg mL^{-1}	0.4605 ng mL^{-1}	human serum	[7]
Fluorescence	AIE/AuNCs	0.01–100 μg mL^{-1}	2.79 ng mL^{-1}	serum	this study

E-AB (electrochemical aptamer-based), HPLC (High-performance liquid chromatography), LC-MS (Liquid chromatography mass spectrometry), DFPA (Direct Fluorescence Polarization Assay), AIE (aggregation-induced emission).

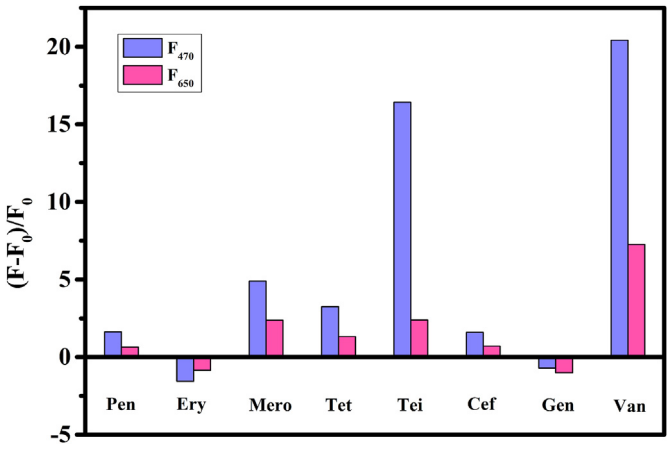

Fig. 5. Evaluation of selectivity towards various antibiotics. The Van concentration was 10 μg mL^{-1}, while that of the other antibiotics was 100 μg mL^{-1}.

types of antibiotics were evaluated, including penicillin (Pen), erythromycin (Ery), meropenem (Mero) tetracycline (Tet), teicoplanin (Tei), ceftazidime (Cef), and gentamicin (Gen). The fluorescence signals for Van at 10 μg mL^{-1} and other antibiotics at 100 μg mL^{-1} were shown in Fig. 5. For other antibiotics, the fluorescence intensity did not significantly increase, except for Tei at 470 nm. Van and Tei are glycopeptide antibiotics with similar structures and are able to specifically interact with the D-Ala-D-Ala short peptide; accordingly, they could be detected by TPE-p simultaneously. However, TPE-p and Van aptamer only responded to Van and not to Tei. These results indicated that the high selectivity of the dual-emission method was sufficient for Van detection.

3.6. Analytical application

To further evaluate the feasibility of the biosensor platform for the analysis of real samples, serum samples were spiked with various concentrations of Van (1, 5, 10, 20, and 50 μg mL^{-1}). As shown in Table 2, Van recoveries were in the range of 98–105% and RSD values were <5.8%. To further explore the accuracy and precision, the results of our newly developed method were compared with those of ELISA by a Passing & Bablok regression analysis. As shown in Fig. 6A, the results for the two detection methods were highly correlated, with no significant deviation from linearity and a correlation coefficient of 0.98. Plasma concentration–time profiles of three rabbits (Fig. 6B) and the corresponding PK parameters were provided in Table 3. The areas under the curve from 0 h to the last time point (AUC_{0-last}) of three rabbits were 9595, 9546, 7833 min μg mL^{-1}, respectively. The peak drug concentration (C_{max}) and the time to C_{max} (T_{max}) were approximately 40 μg mL^{-1} and 110 min, respectively. The Van half-life ($T_{1/2}$) was approximately

Table 2
Detection of Van in serum samples (n = 4).

Spiked (μg mL^{-1})	Found (μg mL^{-1})	Recovery (%)	RSD (%)
1	1.05	105.0	5.8
5	5.08	101.6	4.1
10	9.80	98.0	4.2
20	20.43	102.2	3.6
50	50.93	101.9	1.9

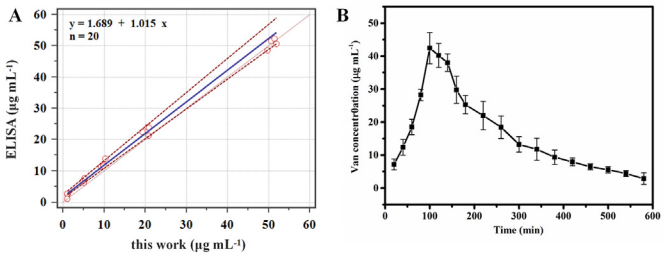

Fig. 6. (A) Method comparison of the Van assays with Passing-Bablok (the present study and ELISA). (B) Mean concentration–time profiles of Van in rabbits.

Table 3
Pharmacokinetic parameters for rabbits.

PK parameter	Rabbit 1	Rabbit 2	Rabbit 3
AUC_{0-last} (min·μg mL^{-1})	9595	9546	7833
C_{max} (μg mL^{-1})	38.9	43.4	36.1
T_{max} (min)	118	113	111
$T_{1/2}$ (min)	262	222	209

3–4 h in these rabbits. These results indicated that our method offers a feasible alternative for the quantitative detection of Van. Furthermore, this method can be used to quantify Van in vivo.

4. Conclusion

This study describes the development of a new dual-emission biosensor platform for the simple, sensitive, and specific detection of Van on the basis of fluorescent peptide-conjugated AIE and aptamer-modified AuNCs. Compared with previously reported Van assays, the method provided both a wide detection range and high selectivity for distinguishing glycopeptide antibiotics owing to the strong affinity towards the peptide and aptamer. The probe could be used to visualize and quantify Van, with an easily observable color change. More broadly, the strategy provides a new approach for the development of sensitive, convenient, and visual detection systems and can expand the practical detection of clinical drug concentrations.

CRediT authorship contribution statement

Fangya Mu: Conceptualization, Methodology, Investigation, Writing - original draft. **Junqing He:** Formal analysis, Investigation, Validation. **Fang Fan:** Investigation, Supervision. **Guoyue Shi:** Conceptualization, Funding acquisition, Methodology, Supervision, Writing - review & editing.

Declaration of competing interest

The authors declare that they have no known competing financial interests or personal relationships that could have appeared to influence the work reported in this article.

Acknowledgments

Funding: This work was supported by the National Natural Science Foundation of China [grant number 21675053]; the Key Project of Science and Technology Commission of Shanghai Municipality [grant number 18DZ1112700]; and the 'Flower of Happiness,' The Special Fund for Pilot Technology of East China Normal University.

Appendix A. Supplementary data

Supplementary data to this article can be found online at https://doi.org/10.1016/j.aca.2020.12.052.

References

[1] R.K. Shields, J.L. Martello, B.A. Potoski, Is vancomycin ototoxicity a significant risk? Antimicrob. Agents Chemother. 53 (2009) 4572.
[2] M.J. Rybak, J. Le, T.P. Lodise, D.P. Levine, J.S. Bradley, C. Liu, B.A. Mueller, M.P. Pai, A. Wong-Beringer, J.C. Rotschafer, K.A. Rodvold, H.D. Maples, B.M. Lomaestro, Therapeutic monitoring of vancomycin for serious methicillin-resistant Staphylococcus aureus infections: a revised consensus guideline and review by the American Society of Health-System Pharmacists, the Infectious Diseases Society of America, the Pediatr, Am. J. Health Syst. Pharm. 77 (2020) 835–864.
[3] L. Javorska, L.K. Krcmova, D. Solichova, P. Solich, M. Kaska, Modern methods for vancomycin determination in biological fluids by methods based on high-performance liquid chromatography - a review, J. Separ. Sci. 39 (2016) 6–20.
[4] P. Milla, F. Ferrari, E. Muntoni, M. Sartori, C. Ronco, S. Arpicco, Validation of a simple and economic HPLC-UV method for the simultaneous determination of vancomycin, meropenem, piperacillin and tazobactam in plasma samples, J. Chromatogr. B. 1148 (2020) 122151.
[5] I. Chianella, A. Guerreiro, E. Moczko, J.S. Caygill, E.V. Piletska, I.M.P. De Vargas Sansalvador, M.J. Whitcombe, S.A. Piletsky, Direct replacement of antibodies with molecularly imprinted polymer nanoparticles in ELISA - development of a novel assay for vancomycin, Anal. Chem. 85 (2013) 8462–8468.
[6] L. Yu, M. Zhong, Y. Wei, Direct fluorescence polarization assay for the detection of glycopeptide antibiotics, Anal. Chem. 82 (2010) 7044–7048.
[7] W. Liang, S. Liu, Z. Liu, D. Li, L. Wang, C. Hao, Y. He, Electron transfer and fluorescence "turn-off" based CdTe quantum dots for vancomycin detection at nanogram level in aqueous serum media, New J. Chem. 39 (2015) 4774–4782.
[8] P. Dauphin-Ducharme, K. Yang, N. Arroyo-Currás, K.L. Ploense, Y. Zhang, J. Gerson, M. Kurnik, T.E. Kippin, M.N. Stojanovic, K.W. Plaxco, Electrochemical aptamer-based sensors for improved therapeutic drug monitoring and high-precision, feedback-controlled drug delivery, ACS Sens. 4 (2019) 2832–2837.
[9] K.S. Park, M. Il Kim, M.A. Woo, H.G. Park, A label-free method for detecting biological thiols based on blocking of Hg^{2+}-quenching of fluorescent gold nanoclusters, Biosens. Bioelectron. 45 (2013) 65–69.
[10] N.L. Rosi, C.A. Mirkin, Nanostructures in biodiagnostics, Chem. Rev. 105 (2005) 1547–1562.
[11] I.M. Khan, S. Niazi, Y. Yu, A. Mohsin, B.S. Mushtaq, M.W. Iqbal, A. Rehman, W. Akhtar, Z. Wang, Aptamer induced multicolored AuNCs-WS_2 "turn on" FRET nano platform for dual-color simultaneous Detection of AflatoxinB1 and Zearalenone, Anal. Chem. 91 (2019) 14085–14092.
[12] W.Y. Chen, G.Y. Lan, H.T. Chang, Use of fluorescent DNA-templated gold/silver nanoclusters for the detection of sulfide ions, Anal. Chem. 83 (2011) 9450–9455.
[13] S. Xu, X. Feng, T. Gao, G. Liu, Y. Mao, J. Lin, X. Yu, X. Luo, Aptamer induced multicoloured Au NCs-MoS_2 "switch on" fluorescence resonance energy transfer biosensor for dual color simultaneous detection of multiple tumor markers by single wavelength excitation, Anal. Chim. Acta 983 (2017) 173–180.
[14] J. Luo, Z. Xie, Z. Xie, J.W.Y. Lam, L. Cheng, H. Chen, C. Qiu, H.S. Kwok, X. Zhan, Y. Liu, D. Zhu, B.Z. Tang, Aggregation-induced emission of 1-methyl-1,2,3,4,5-pentaphenylsilole, Chem. Commun. 18 (2001) 1740–1741.
[15] J. Mei, Y. Huang, H. Tian, Progress and trends in AIE-based bioprobes: a brief Overview, ACS Appl. Mater. Interfaces 10 (2018) 12217–12261.
[16] H. Shi, R.T.K. Kwok, J. Liu, B. Xing, B.Z. Tang, B. Liu, Real-time monitoring of cell apoptosis and drug screening using fluorescent light-up probe with aggregation-induced emission characteristics, J. Am. Chem. Soc. 134 (2012) 17972–17981.
[17] H. Shi, J. Liu, J. Geng, B.Z. Tang, B. Liu, Specific detection of integrin α vβ 3 by light-up bioprobe with aggregation-induced emission characteristics, J. Am. Chem. Soc. 134 (2012) 9569–9572.
[18] F. Hu, B. Liu, Organelle-specific bioprobes based on fluorogens with aggregation-induced emission (AIE) characteristics, Org. Biomol. Chem. 14 (2016) 9931–9944.
[19] D. Ding, C.C. Goh, G. Feng, Z. Zhao, J. Liu, R. Liu, N. Tomczak, J. Geng, B.Z. Tang, L.G. Ng, B. Liu, Ultrabright organic dots with aggregation-induced emission characteristics for real-time two-photon intravital vasculature imaging, Adv. Mater. 25 (2013) 6083–6088.
[20] J. Xie, Y. Zheng, J.Y. Ying, Protein-directed synthesis of highly fluorescent gold nanoclusters, J. Am. Chem. Soc. 131 (2009) 888–889.
[21] S. Gao, G. Wei, S. Zhang, B. Zheng, J. Xu, G. Chen, M. Li, S. Song, W. Fu, Z. Xiao, W. Lu, Albumin tailoring fluorescence and photothermal conversion effect of near-infrared-II fluorophore with aggregation-induced emission characteristics, Nat. Commun. 10 (2019) 2206.
[22] M. Wang, J. Chen, D. Su, G. Wang, X. Su, Split aptamer based sensing platform for adenosine deaminase detection by fluorescence resonance energy transfer, Talanta 198 (2019) 1–7.
[23] S.G. Wicha, C. Kloft, Simultaneous determination and stability studies of linezolid, meropenem and vancomycin in bacterial growth medium by high-performance liquid chromatography, J. Chromatogr. B. 1028 (2016) 242–248.
[24] M. Oyaert, N. Peersman, D. Kieffer, K. Deiteren, A. Smits, K. Allegaert, I. Spriet, J. van Eldere, J. Verhaegen, P. Vermeersch, S. Pauwels, Novel LC-MS/MS method for plasma vancomycin: comparison with immunoassays and clinical impact, Clin. Chim. Acta 441 (2015) 63–70.
[25] S.M. Ng, X. Wu, M.F. Khyasudeen, P.J. Nowakowski, H.S. Tan, B. Xing, E.K.L. Yeow, Vancomycin determination by disrupting electron-transfer in a fluorescence turn-on squaraine-anthraquinone triad, ACS Sens. 3 (2018) 1156–1163.